Shielded Scintillator for Neutron Characterization

A Thesis Submitted in Partial Fulfillment of the

Requirements for Graduation with Research Distinction in Engineering Physics

By

Patrick X. Belancourt

The Ohio State University

May 17, 2012

Project Advisor:

Dr. Richard R. Freeman, Department of Physics

Abstract

The High Energy Density Physics group is studying the basic science of a novel neutron and gamma ray source for the Defense Threat Reduction Agency to probe nuclear material nondestructively. The neutrons and gamma rays are produced by accelerating ions via a laser into a target and creating fusion neutrons and gamma rays. A scintillator will be used as a time of flight detector to characterize the neutron source. Neutrons and photons produce ionizing radiation in the scintillator which then activates metastable states. These metastable states have both short and long decay rates. The initial photon count is orders of magnitude higher than the neutron count and poses problems for accurately detecting the neutrons due to the long decay state that is activated by the photons. Shielding the scintillator with lead will attenuate the photons but could also delay and scatter the neutrons. A Monte Carlo transport code was used to determine the feasibility of using a shielded scintillator as a time of flight detector. It was found that shielding the scintillator with 5-7 cm of lead is optimal.

Table of Contents

List of Figures

1. Introduction

The proliferation of special nuclear materials is a key concern of the United States. Traditionally to combat proliferation, cargo is scanned with X-rays for isotopes of interest. However if the cargo is shielded in a high Z material, such as lead, then a X-ray scanner may not be able to detect such materials. High energy neutrons are able to pass through lead with most of their initial energy. When the neutron interacts with the special nuclear material, characteristic radiation is given off that can be detected[1].

As part of the High Energy Density Physics Group at the Ohio State University, I am interested in investigating the basic science of creating a high energy neutron and gamma ray source from a high intensity, short pulsed laser. In preparation for creating neutrons, the feasibility of using a scintillator shielded with lead was explored for characterization of neutron energies.

1.1 Basic Science of Creating High Energy Neutrons and Gamma Rays

Neutron and gamma rays will be produced via laser-matter interaction. A high intensity laser that shines on a thin metal target transfers some of its energy to the electrons in the metal[2]. The electrons are accelerated to relativistic speeds in the target. Due to the electrons being accelerated through the target, there is a huge charge separation in the target. Huge electric fields are generated from the charge separation that

confines the majority of the electrons to the target. These electrons slow down partially by the bremsstrahlung interaction, which emits a photon in the direction of the traveling electron[3]. These high energy gamma rays are the first part of the gamma ray-neutron source.

The charge separation of the refluxing electrons and the target induce very high electric fields. These electric fields accelerate the ions on the surface of the thin metal target, with most of the ions being accelerated from the rear surface of the target[2-4]. By applying a layer of heavy water or deuterated plastic to back of the targets, deuterium ion acceleration is possible[5]. Placing another deuterated target directly behind the first target, allows the accelerated deuterium ions to interact with the second deuterated target[6]. The overall process is shown schematically in figure 1. The resulting Deuteron-Deuteron interaction has a chance of fusing, isotropically emitting a 2.45 MeV neutron in the center of mass frame. These 2.45 MeV neutrons are the second part of the gamma ray-neutron source.

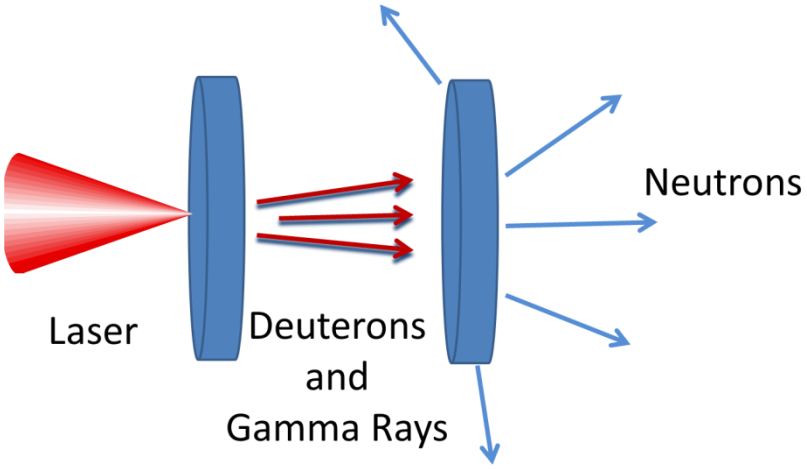

Figure 1: Basic schematic of creating high energy gamma rays and neutrons

2. Plastic Scintillator Physics

To characterize the neutron source in terms of neutron energy distribution, a plastic scintillator can be used as a time of flight detector. A time of flight detector is able to give the energy of the neutrons from basic kinematics. Since the distance from the source to the detector is known and fixed and the neutrons are nonrelativistic, then measuring the time it takes the neutron to reach the detector will yield the neutron's energy according to equation 1.

$$E = \frac{m_{neutron}}{2}\left[\frac{distance}{\Delta t}\right]^2 \qquad (1)$$

Plastic scintillators are sensitive to both neutrons and photons. Neutrons interact with the hydrogen in the plastic to knock out a proton. This proton activates metastable states of the scintillator. These metastable states decay and emit a photon. The photon interacts with the electrons in the scintillator. A fraction of the photons collected by the photo-cathode of the photomultiplier tube generate electrons which are amplified and the resulting signal is sent to an oscilloscope[7]. A visual representation is shown in figure 2.

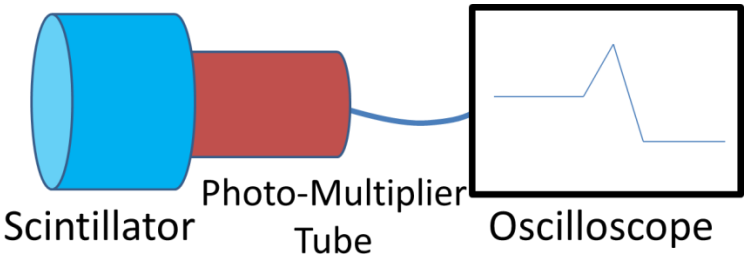

Figure 2: Components of scintillator detector

2.1 Shielding of Plastic Scintillator

The x-rays produced by the same laser-matter interaction that accelerates the ions reach the scintillator at the speed of light. The neutrons, which are traveling much less than the speed of light, arrive at the scintillator later in time. Since the scintillator has many other decay states, the scintillator continues to glow from the initial x-ray

interactions when the neutrons reach the scintillator[8]. The total number of neutrons produced is orders of magnitude less than the total x-ray production, so the neutron signal could be convoluted from the continuing emission from the initial x-rays interaction. From simulation results[9], it has been shown that about 1% of the laser energy is converted to x-ray energy. Assuming that the x-ray energy distribution is a Maxwell-Boltzmann distribution with an average energy of 1.5 MeV, and then the number of x-rays produced per joule of laser energy is 8.4E11. This is orders of magnitude higher than the maximum neutron production per joule of laser energy[5]. Figure 3 shows a cartoon illustration of what the output of the oscilloscope is expected to look like. To get a better resolution of the neutron signal, the scintillator will have to be shielded to reduce the number of x-rays reaching the scintillator.

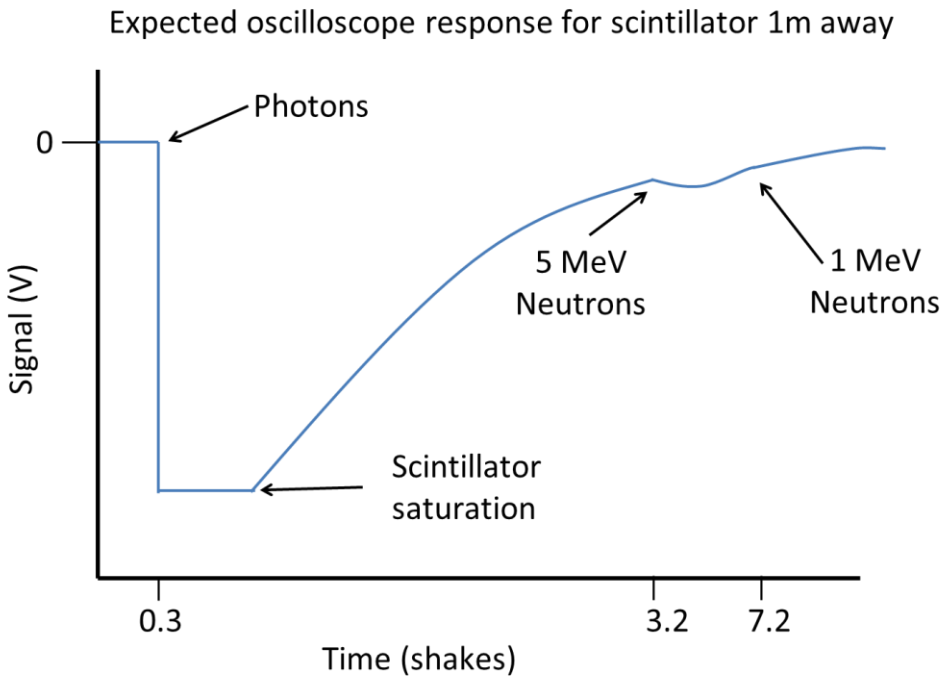

Figure 3: Pictorial representation of expected oscilloscope output

High Z materials are effective at attenuating x-rays. Equation 2 gives a simple formula for the attenuation of monoenergetic x-rays through matter. I_0 is the initial intensity of the x-rays, μ is the linear attenuation coefficient, which depends on the material the x-rays are passing through and the energy of the x-rays and x is the thickness of the shield. Lead has been chosen to be investigated as the shielding material due to cost and availability.

$$I(x) = I_0 * e^{-\mu * x} \quad (2)$$

Neutrons lose very little energy when elastically scattering though high z materials due to the large mass difference between the nucleus and incoming neutron[10]. Neutrons can have a variable amount of scattering in the lead which in turn leads to a variable amount of time it would take for the neutron to reach the scintillator. Figure 4 shows a cartoon of this process. Increasing the thickness of the lead shield increases the number of potential scattering events. If there is a wide spread of number of scattering events it will lead to neutrons of the same energy reaching the scintillator at a variable time range. Since the time of flight principle is based off of knowing exactly the time it takes for the neutron to reach the detector, this scattering could reduce the usefulness of the time of flight detector. Also even though neutrons do not lose much energy in elastic collisions with lead, they still scatter at various angles. This could lead to a lower amount of neutrons reaching the scintillator, which does not contribute to the overall goal of improving the resolution of the neutron signal on the oscilloscope.

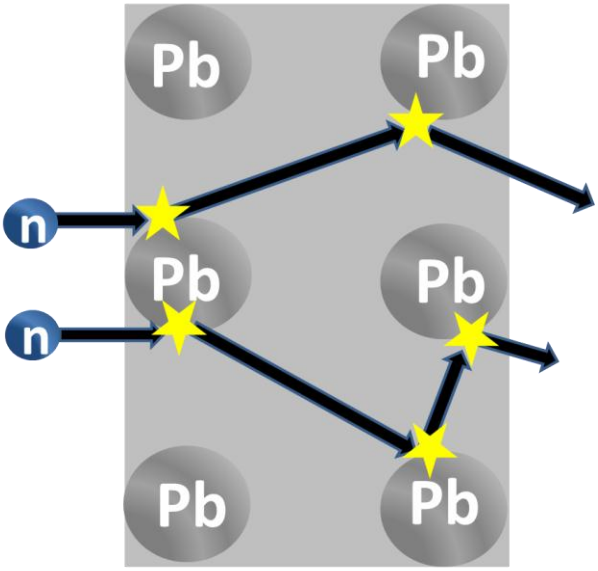

Figure 4: Illustration of neutrons scattering through lead

3. MCNP5

To determine the effect on the transport of neutrons and photons by adding a lead shield around the scintillator, the Monte Carlo N-Particle (MCNP5) code was used[11]. MCNP5 is a Monte Carlo code that calculates the transport of particles one at a time. The code then runs many particles and averages the results to obtain statistics of what an average particle will do. To setup a MCNP5 simulation, the user inputs the 3D geometry by specifying planes and macrobodies and using Boolean operators to join them. The user has full control on the specification of the source and is able to extract useful information from the simulation such as flux and energy deposition through tally cards. These tally

cards can be binned according to energy, time and angle that the particle crossed a plane at.

4. Methodology

4.1 Simulation Geometry

The basic elements of the control room were modeled, including the concrete floor, the aluminum target chamber and the actual detector set up as shown in figure 5. The target chamber was approximated as spherical shell with a wall thickness of 5 cm and an inside radius of 48.34 cm. At the center of the target chamber is the photon or neutron source particles with vacuum everywhere else in the target chamber. The target chamber is located 129.54 cm off the concrete floor. The concrete floor has a thickness of 13.7 cm and spans the bottom of the entire simulation.

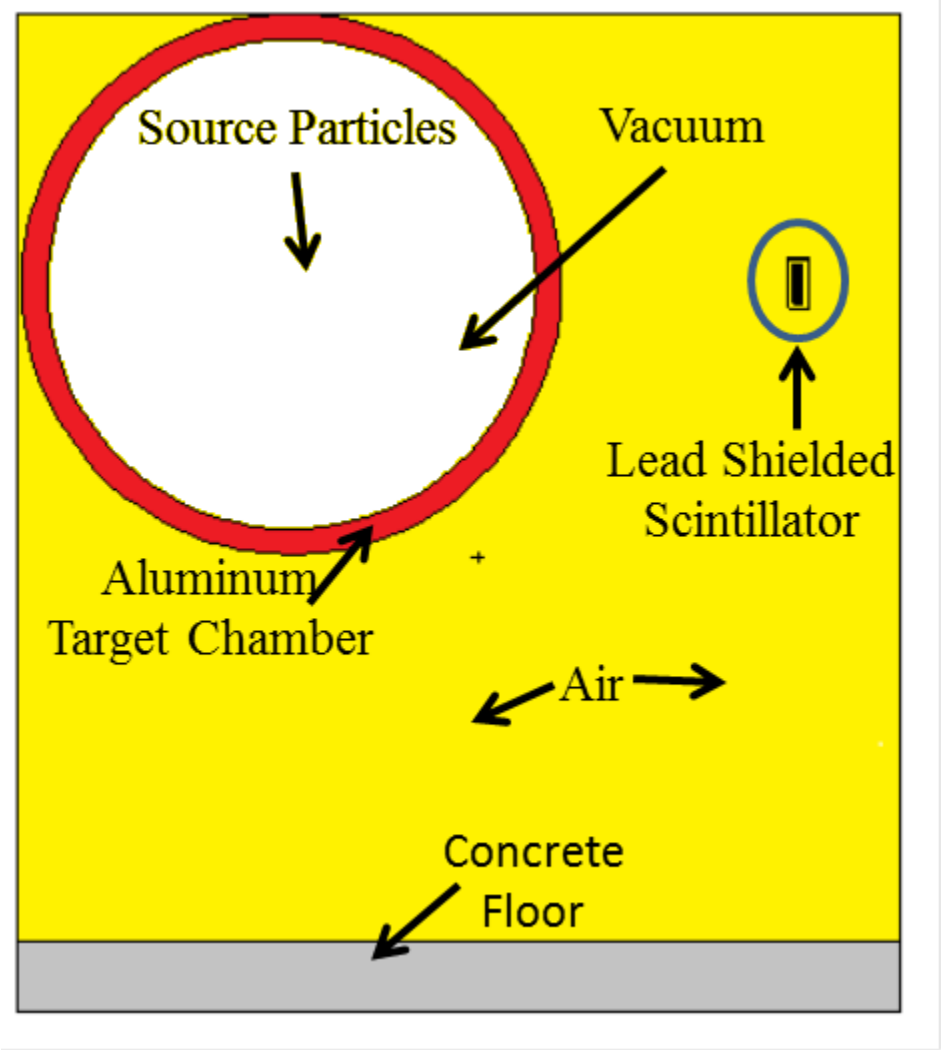

Figure 5: Cross sectional view of simulation geometry

The lead shielded scintillator setup is located 1m away from the source particles in the x direction. The scintillator is modeled as a plastic puck, with a radius of 4 cm and a thickness of 2 cm. Figure 6 shows the box type configuration of the lead shielding, which is a lead cube shell with a variable thickness. Figure 7 shows the wall type configuration, which has a variable thickness of lead facing the particle source, and a

constant thickness of 0.1 cm of lead elsewhere. There is a constant 1 cm of air in between the lead shielding and plastic scintillator for both configurations.

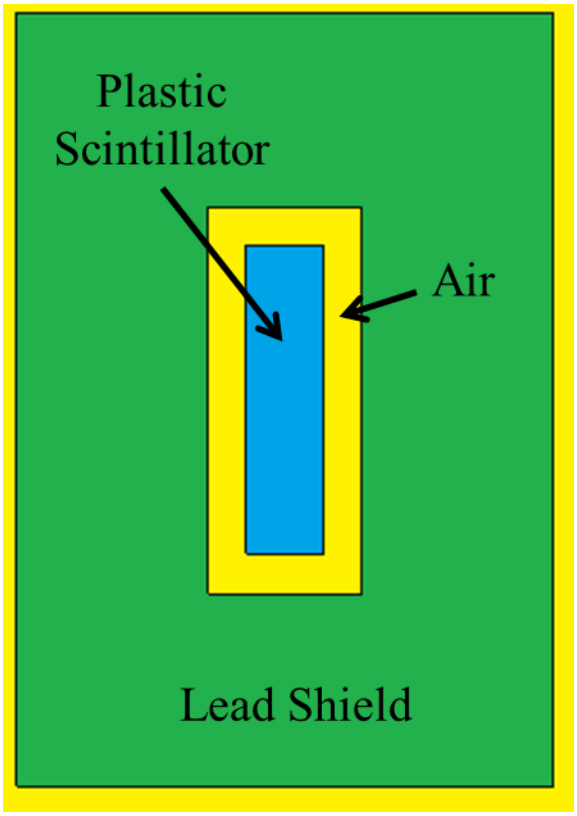

Figure 6: Cross sectional view of lead shielded scintillator setup in box configuration

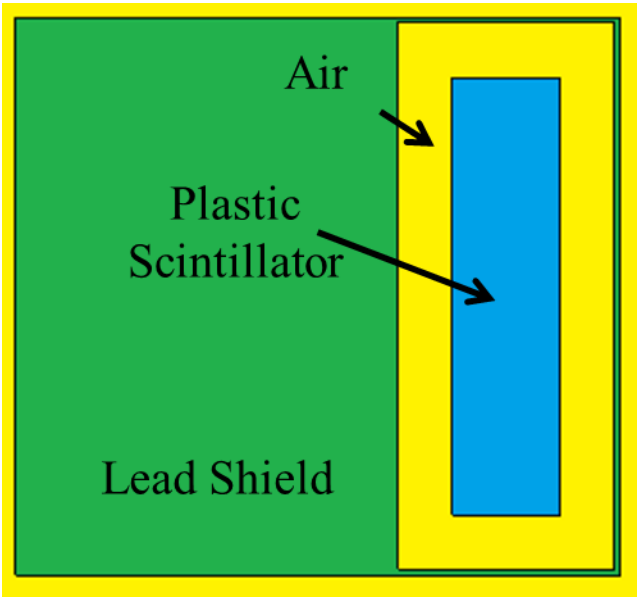

Figure 7: Cross sectional view of lead shielded scintillator setup in wall configuration

4.2 Neutron and Photon Source Specifications

The neutron source was approximated to be a point source in the middle of the target chamber. In order to determine how the energy deposition rate in the scintillator changes as a function of energy, monoenergetic neutrons were used. 1 MeV, 2.45 MeV and 6 MeV neutrons were used. The neutrons were all emitted in the same direction, directly in the line of sight of the detector.

The energy deposition card (F6) was the main tally used in the simulation to determine energy deposition within the scintillator. The tally was binned according to the

energy (e0) of the neutron that deposited the energy, the time it took for the neutron to make it to the scintillator and deposit energy and the location in the scintillator where the energy was deposited. The specific energy binning was dependent on the initial energy of the neutrons used in the simulation but as a general rule the bin resolution was finer near the initial energy of the neutron. The time card (t0) was also heavily dependent on the initial neutron energy. The time cards were made so that the time interval between when a neutron would first enter the scintillator and exit the scintillator was binned very finely, about 0.001 shakes. The rest of the time bins broadened as time processed and the simulation itself was ended at 20 shakes.

The photon source was also modeled as a point source in the middle of the target chamber. The photon source had a Maxwell distribution with kT=1MeV. The photons were emitted in a 30 degree, half angle cone, with the probability of being emitted in a given angle controlled by a Lorentzian function.

5. Results and Discussion

The total energy deposition per photon into the plastic scintillator for each simulation was plotted, as shown in figure 8. In order to determine if the lead shielded plastic scintillator could be used as a time of flight detector, the lead thickness had to be optimized for minimum photon signal and still retaining the time of flight qualities for

neutrons. As a first pass, 90% of the photon energy deposition being blocked could make this feasible. From figure 8, the corresponding amount of lead would be somewhere between 5-7 cm.

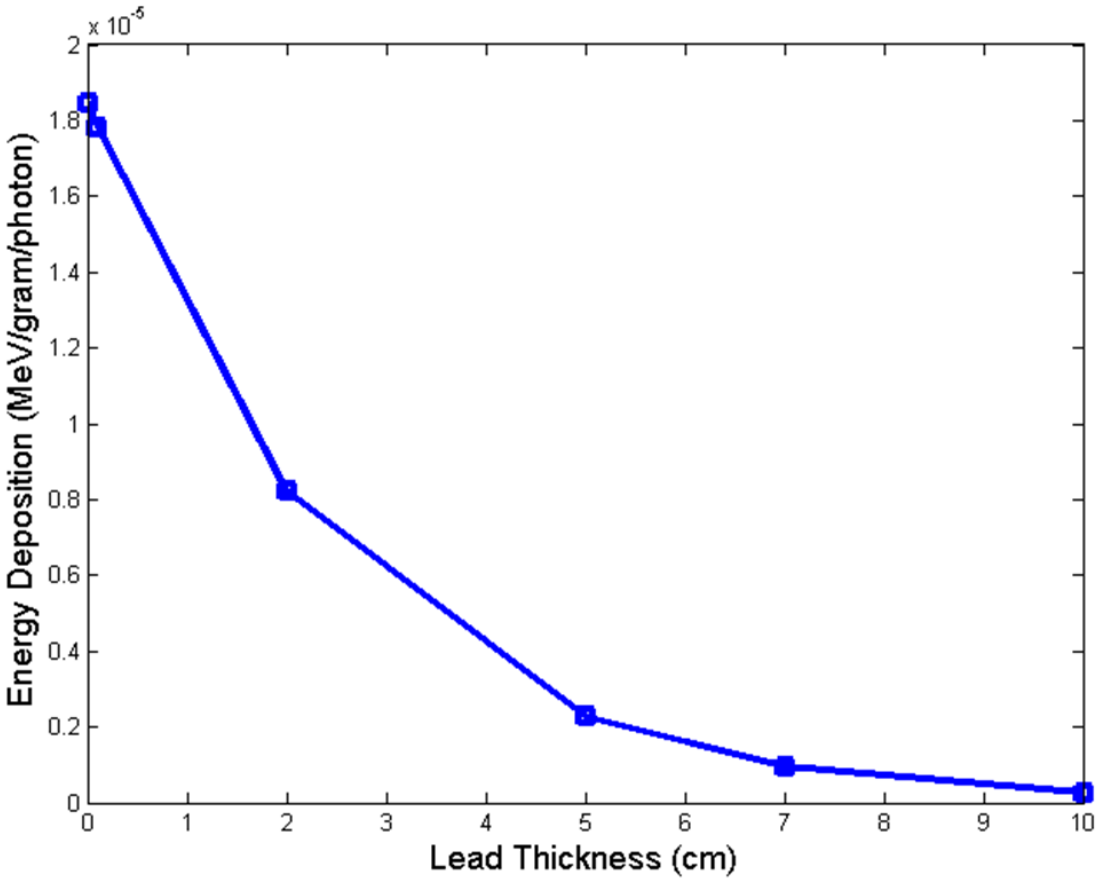

Figure 8: Photon energy deposition for various thickness of lead

To clearly present the vast number of data points associated with the neutron simulations, plots were generated based on lead shielding thickness and initial neutron energy. The data points were divided by their bin width to have a smooth function.

Figure 9 shows the energy deposition rate for 1, 2.45 and 6 MeV neutrons through 5 cm of lead. The first immediate feature that the plot shows is the time of flight feature. The energy deposition rate for neutrons is spread out in time according to their initial energy, with higher energy neutrons arriving at the scintillator before the lower energy neutrons. The width of the signal for each energy corresponds to the amount of time it takes the neutrons of a given energy to travel though the scintillator. The plot also shows the relationship between initial neutron energy and the total energy deposition in the scintillator when a shield is added. Higher energy neutrons are able to penetrate through the lead more and deposit more energy into the scintillator.

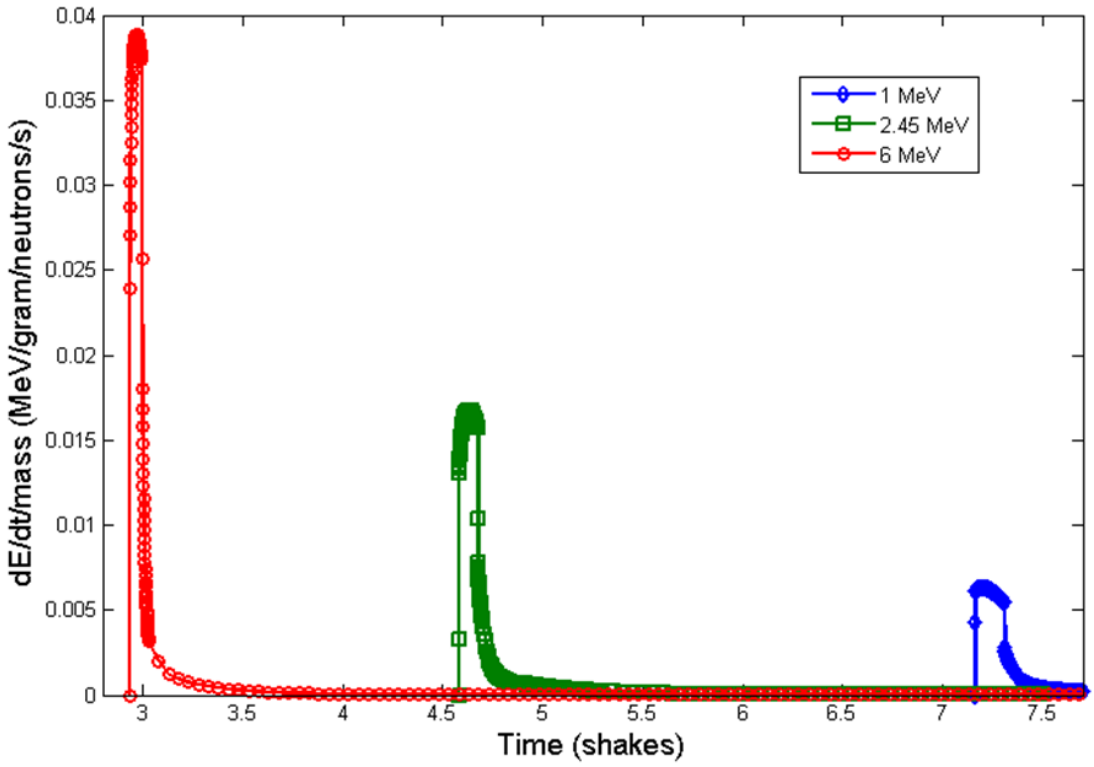

Figure 9: Energy deposition rate for various energy neutrons for 5 cm of lead

The energy deposition rate for 1 MeV neutrons is plotted in figure 10. As expected the total energy deposition in the scintillator decreases as lead shielding thickness is increased. This is due for neutrons scattering off of the lead nucleus and never reaching the scintillator. This plot also shows that there is still energy being deposited into the scintillator at later times. This is due to neutrons scattering back into the scintillator at a later time or neutrons having multiple collisions in the scintillator. Also with increasing lead thickness, the peak energy deposition shifts to later in time.

This is due to neutrons scattering in the lead and then reaching the scintillator. 10 cm of lead shielding appears to be reaching a threshold for significantly decreasing the resolution of the scintillator as a time of flight detector due to the main signal approaching the signal of the tail of the function. Figure 11 and figure 12 shows the energy deposition rate for 2.45 MeV and 6 MeV neutrons, respectively. The higher energy neutrons show the same behavior and characteristics as the 1 MeV neutrons.

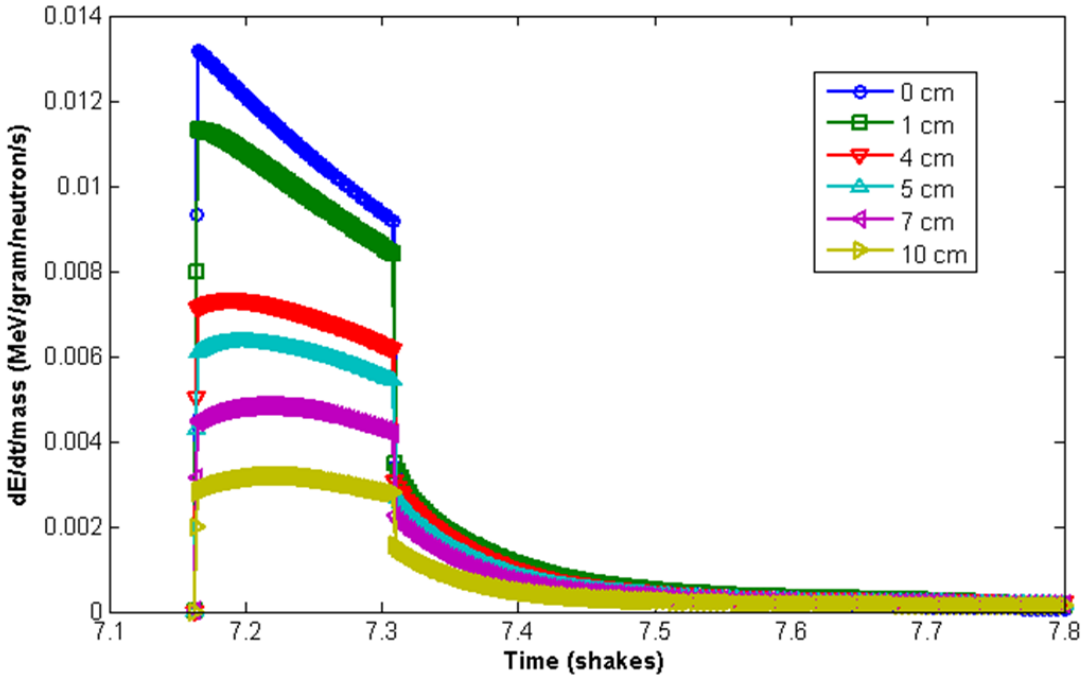

Figure 10: Energy deposition rate for 1 MeV neutrons for various thicknesses of lead

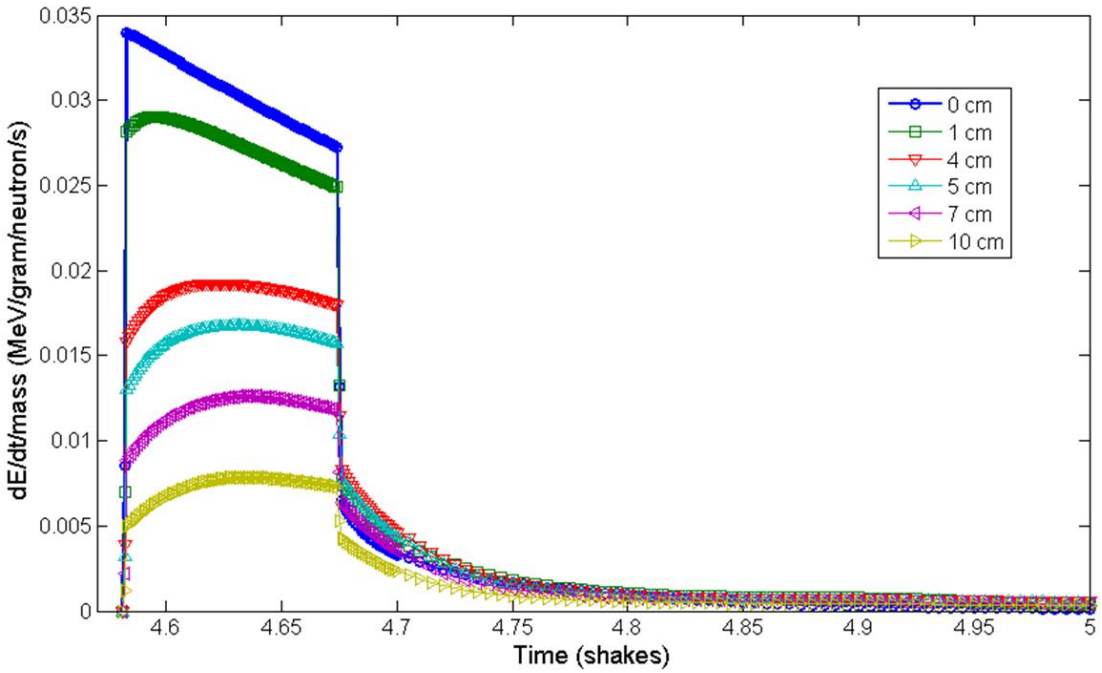

Figure 11: Energy deposition rate for 2.45 MeV neutrons for various thicknesses of lead

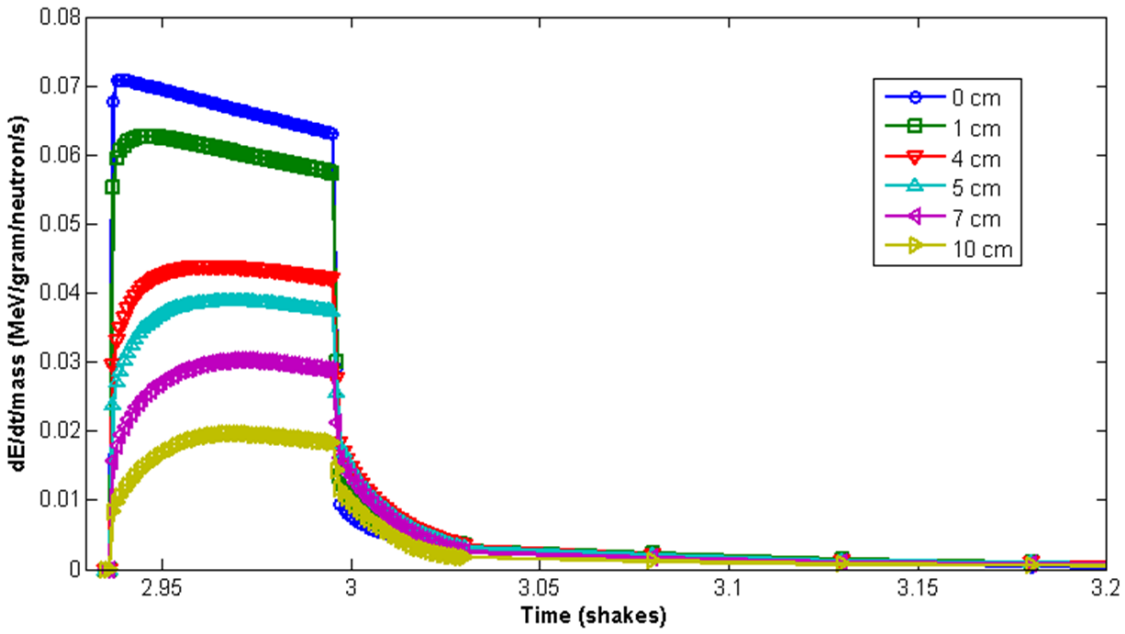

Figure 12: Energy deposition rate for 6 MeV neutrons for various thicknesses of lead

The effect of slightly modifying the geometry of the lead shielding was investigated next. Figure 13 shows the energy deposition rate of 2.45 MeV neutrons for the box and wall type geometry configuration with a lead thickness of 5 cm. The energy deposition rate is exactly the same for the main feature of the curve, indicating that only the lead surface that faces the source plays a role in the initial signal. The only difference of the two geometry appears later in time in the tail of the curve. From the plot it is apparent that scattering of the neutrons back into the scintillator from the sides and back of the lead shield plays a minor role of the signal in the tail. The scattering back in does

not greatly increase the signal in the tail of the function though, which should give some leeway in the experimental setup.

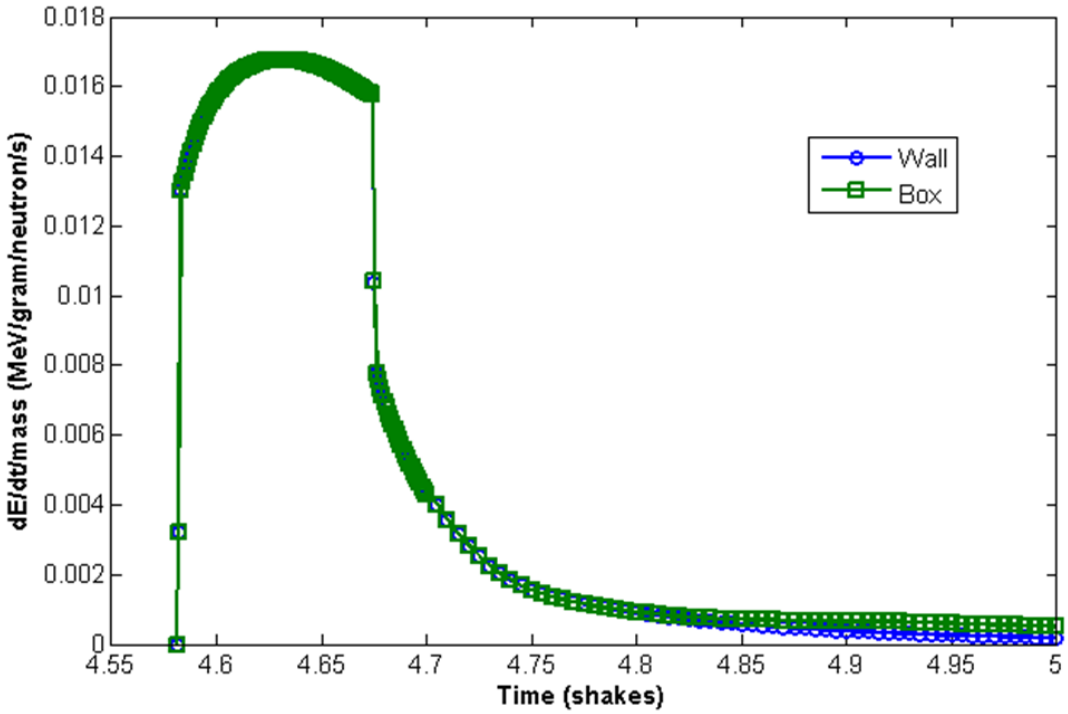

Figure 13: Energy deposition rate for 2.45 MeV through 5 cm of lead for different lead configurations

6. Conclusion

In conclusion, the goal of this project was to determine the feasibility of using a lead shielded scintillator as a time of flight detector for neutron characterization. Adding more lead in front of the detector would prevent more photons from reaching the scintillator but could also decrease the number of neutrons that reach the detector from scattering events in the lead and could interfere with the time of flight principle due to possible ambiguities of the time it takes to reach the detector.

To determine the effects of lead shielding MCNP5, a Monte Carlo, was used to calculate the transport of the neutrons and photons in a simplified geometry resembling possible experimental configuration. The results from the simulations show that a plastic scintillator shielded with 5-7 cm lead can be used as a time of flight detector for fast neutrons. Within this range, the photon energy deposition is decreased by an order of magnitude while the neutron energy deposition is only decreased by a factor of 2 to 3.

7. References

1. Slaughter, D. et al. Detection of Special Nuclear Material in Cargo Containers Using Neutron Interrogation. LLNL, Livermore, CA (2003) UCRL-ID-155315.
2. Hatchet, S. P. et al. Electron, photon, and ion beams from the relativistic interaction of Petawatt laser pulses with solid target. *Phys. Plasmas* **7**, 2076 (2000).
3. Wilks, S. C. et al. Energetic proton generation in ultra-intense laser–solid interactions. *Phys. Plasmas* **8**, 542 (2001).
4. Snavely, R. A. et al. Intense High-Energy Proton Beams from Petawatt-Laser Irradiation of Solids. *Physical Review Letters* **85**, 2945 (2000).
5. Morrison, J. T. et al. Selective deuteron production using target normal sheath acceleration. *Phys. Plasmas* **19**, 030707 (2012).
6. Willingale, l. et al. Comparison of bulk and pitcher-catcher targets for laser-driven neutron production. *Phys. Plasmas* **18**, 083106 (2011).
7. Loveland, W., Morrissey, D., Seaborg, G. Modern Nuclear Chemistry. Place: Wiley, 2001.
8. Lauck, R. et al. Low-Afterglow, High-Refractive-Index Liquid Scintillators for Fast-Neutron Spectrometry and Imaging Applications. *Nuclear Science, IEEE Tans*. **56**, 989 (2009).
9. Private conversation with Andrew Krygier.

10. Lamarsh, J., Baratta, A. Introduction the Nuclear Engineering. Prentice Hall, 2001.
11. X-5 Monte Carlo Team, MCNP–A General Monte Carlo N-Particle Transport Code, Version 5 - Volume II: User's Guide, Los Alamos National Laboratory report LA-CP-03-0245 (2003, Revised 2008)